

Proteomic and phosphoproteomic analyses reveal hyperactive phenotype of platelets in humanized K18-ACE2 mice infected with SARS-CoV-2

Saravanan Subramaniam¹, Ryan Matthew Hekman², Archana Jayaraman¹, Aoife Kateri O'Connell^{3,4}, Paige Montanaro^{3,5}, Devin Kenney^{3,4}, Maria Ericsson⁶, Sarah Walachowski¹, Benjamin Blum², Katya Ravid^{7,8}, Nicholas A Crossland^{3,5}, Florian Douam^{3,4}, Andrew Emili², Markus Bosmann^{1,3,9}



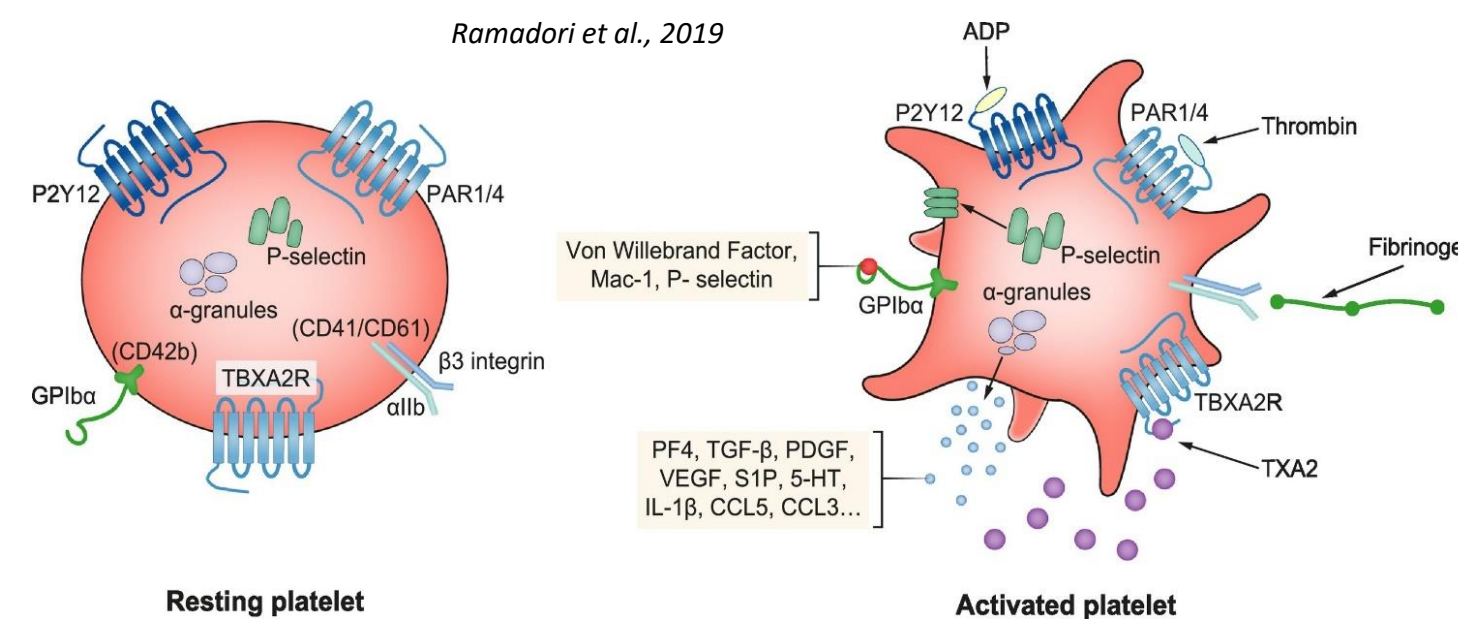
¹Boston University, Department of Medicine, MA, USA; ²Center for Network Systems Biology, Boston University, Boston, MA, USA; ³Boston University, National Emerging Infectious Diseases Laboratories (NEIDL), Boston MA, USA; ⁴Boston University, Department of Microbiology, Boston, MA, USA; ⁵Boston University, Department of Pathology and Laboratory Medicine, Boston, MA, USA; ⁶Electron Microscopy Core Facility, Harvard Medical School, Boston, MA, USA; ⁷Department of Medicine, Boston University School of Medicine, Boston, MA, USA; ⁸Whitaker Cardiovascular Institute, Boston University School of Medicine, Boston, MA, USA; ⁹Center for Thrombosis and Hemostasis, University Medical Center of the Johannes Gutenberg-University, Mainz, Germany

Boston University School of Medicine Pulmonary Center

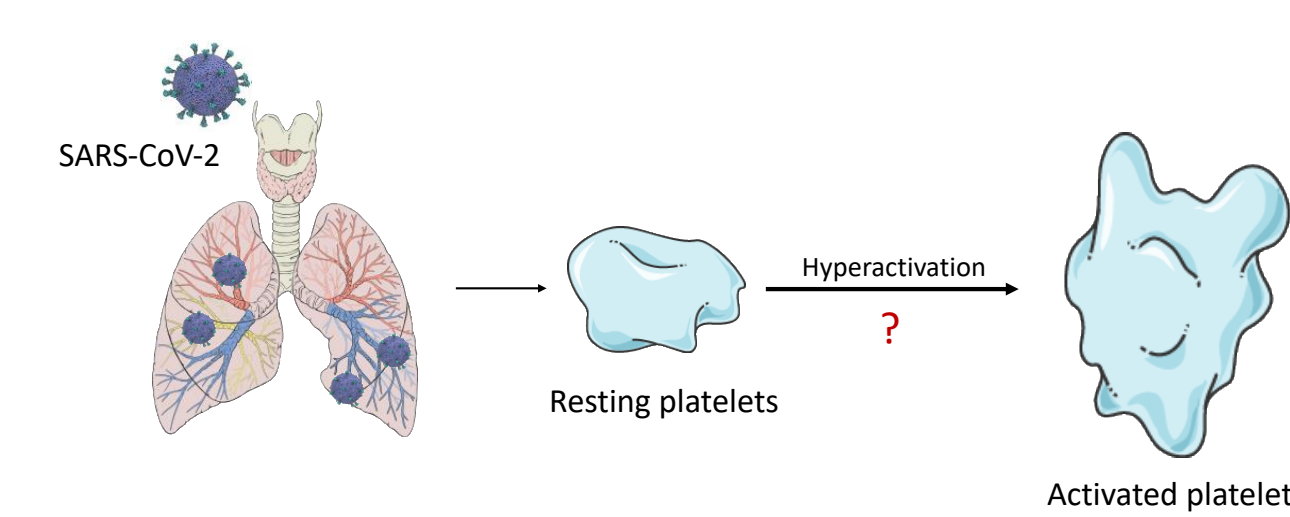
INTRODUCTION

- Coronavirus disease 2019 (COVID-19) is associated with a hypercoagulable state and increased incidence of cardiovascular complications.
- Platelets are effectors of hemostasis and play a major role in coordinating immune and inflammatory activities.
- Suitable animal models are needed to study COVID-19-associated coagulopathy (CAC) and platelet effector functions in COVID-19, which remain largely unclear.
- In our current study, we aimed to characterize alterations in platelets isolated from K18-hACE2 transgenic mice infected with SARS-CoV-2.

Schematic representation of a platelet in its resting state and upon activation: Platelets present membrane G-protein coupled receptors on their surface that can bind several ligands resulting in decreased intracellular cAMP, mobilization of Ca²⁺ stores and subsequent changes of cell morphology. Upon activation, soluble proteins retained in the granules are released via exocytosis, exerting their biological functions in an autocrine or paracrine manner. Similarly, membrane proteins retained in the granules are mobilized and presented at the cellular surface where they can bind related ligands. 5HT, 5-hydroxytryptamine; CCL2, chemokine ligand 2; CCL5, chemokine ligand 5; GPIIb/IIIa, glycoprotein IIb/IIIa; IL-1 β , interleukin-1 β ; PDGF, platelet-derived growth factor; PF4, platelet factor 4; S1P, sphingosine-1-phosphate; TGF- β , transforming growth factor- β ; TXA2, thromboxane A2; VEGF, vascular endothelial growth factor.

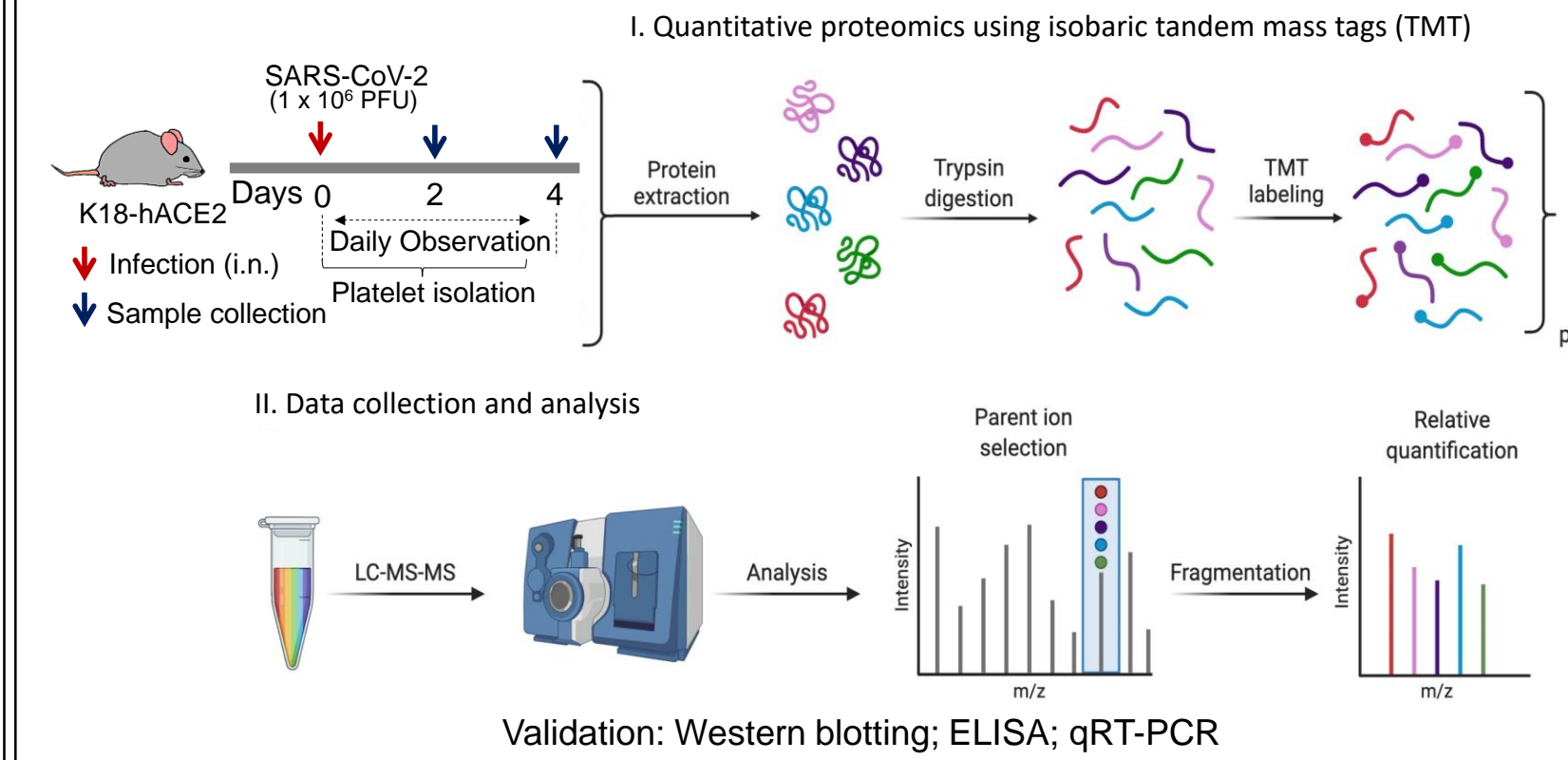


AIM(S)



1. Does SARS-CoV-2 infect platelets?
2. Understand the phenotypic changes in circulating platelets after SARS-CoV-2 infection by MS-based proteomic approach.

METHOD(S)



CONCLUSION(S)

- Abundance of SARS-CoV-2 spike protein in lungs of infected K18-hACE2 mice, but not in platelets and other organs (kidneys), suggests that platelet re-programming towards activation-degranulation-aggregation is likely attributable to a pneumonia-induced elevated circulatory factors (e.g., cytokines and thrombin)-driven response rather than direct platelet infection.
- Complement / coagulation pathways and a hyperactive platelet phenotype re dominant at 2-dpi and interferon signaling is dominant at 4-dpi.
- Circulating platelets in SARS-CoV-2 infected K18-hACE2 mice demonstrate a specific early hyperactive phenotype consistent with procoagulant platelets.

RESULTS

Clinical decline of SARS-CoV-2-infected humanized ACE2 mice

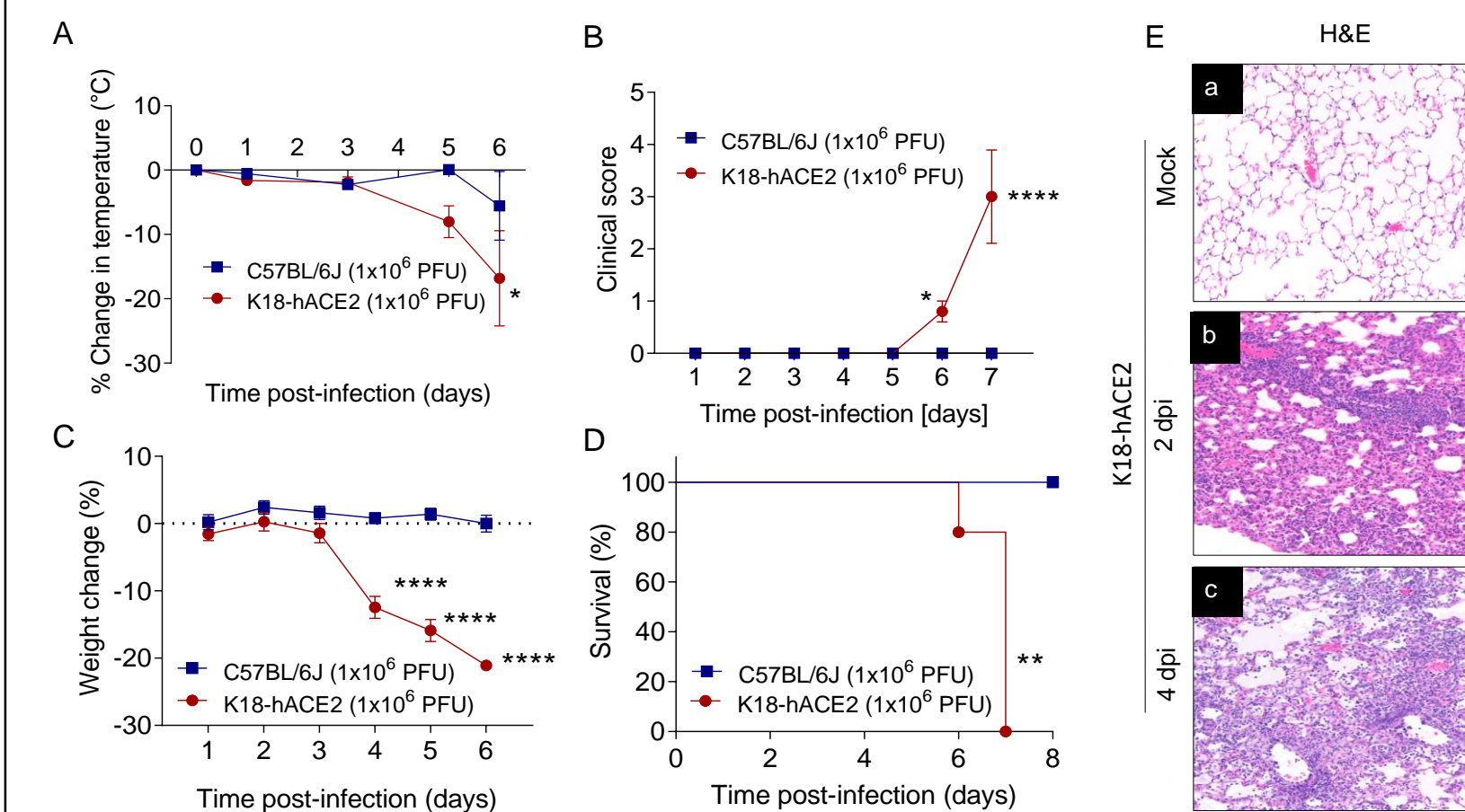


Figure 1. Clinical decline of SARS-CoV-2-infected humanized ACE2 mice. K18-hACE2 mice and C57BL/6J mice were inoculated intranasally with 1×10^6 plaque-forming units (PFU) or received saline (mock). (A) % change in body temperature, (B) clinical score, (C) % change in body weight, and (D) survival were monitored. (E^{a,b,c}) Progressive interstitial pneumonia in K18-hACE2 mice at 2dpi and 4dpi with SARS-CoV-2. H&E staining. Data are shown as the mean \pm SEM, n=5 mice/group *P < .05; **P < .01; ***P < .0001.

Invasive viral load and ultrastructural findings of lung cross sections

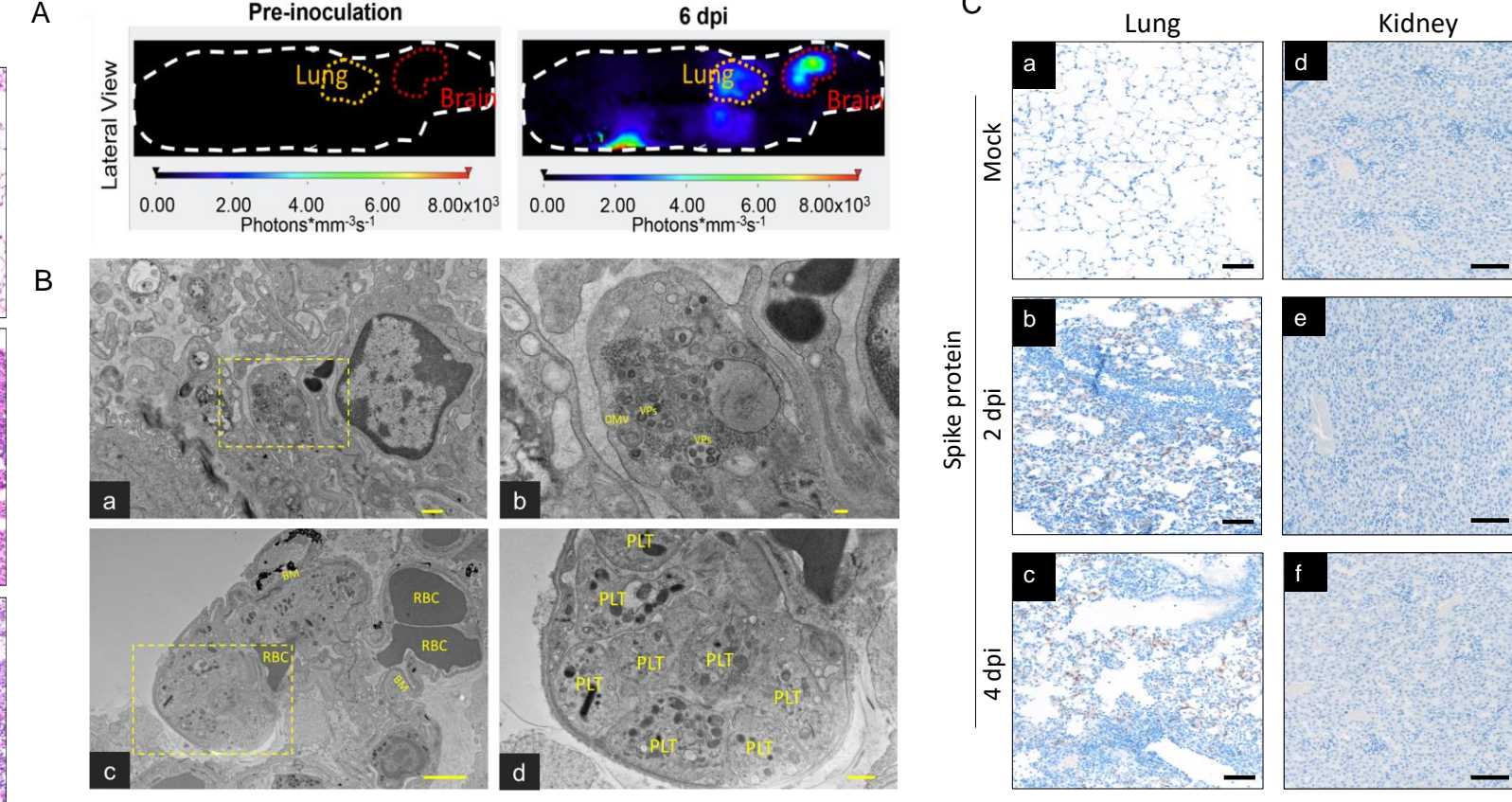


Figure 3. Invasive viral load and ultrastructural findings of lung cross sections. Three-dimensional profile view of a K18-hACE2 mouse following SARS-CoV-2 NL virus (10^6 PFU) infection. NanoLuc bioluminescence signal was quantified at 6 dpi following fluorouracil injection (Sub-cutaneous) using the InVivoPLOT system (Carosino et al., 2022). Location of the lungs and brain are indicated. (B^{a,b}) Viral assembly within an alveolar type I pneumocyte as evidenced by presence of double membrane-bound vesicles (DMVs) that routinely contain viral particles (VPs), transmission electron microscopy. (B^{c-d}) Interstitial capillaries adjacent to areas of viral assembly commonly containing aggregates of platelets at 6dpi. RBC: red blood cells; BM: basement membrane; Scale bars in frames B^{a-d}: a=500 nm; b=100 nm; c=2 μ m; d=500 nm.

Proteome

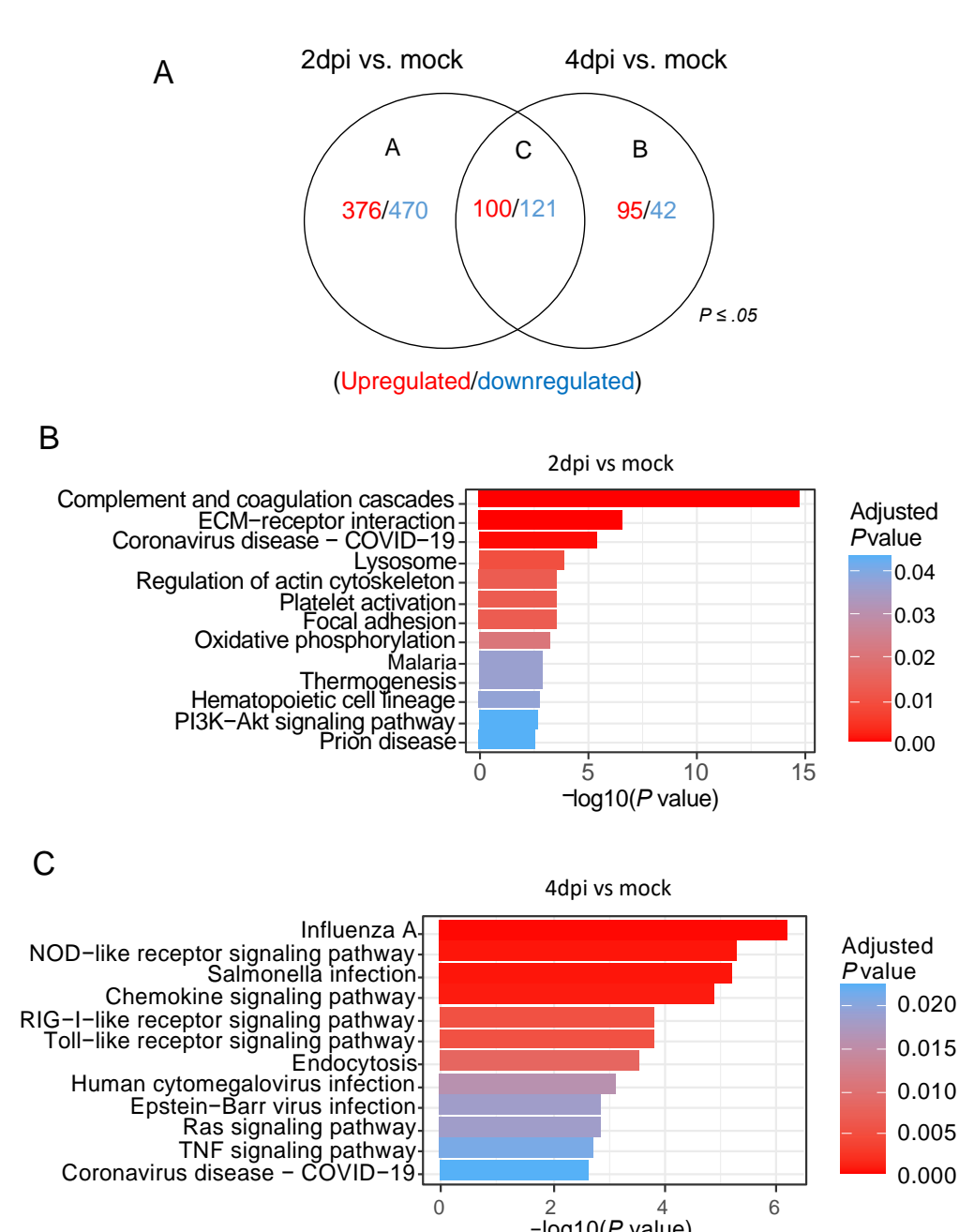
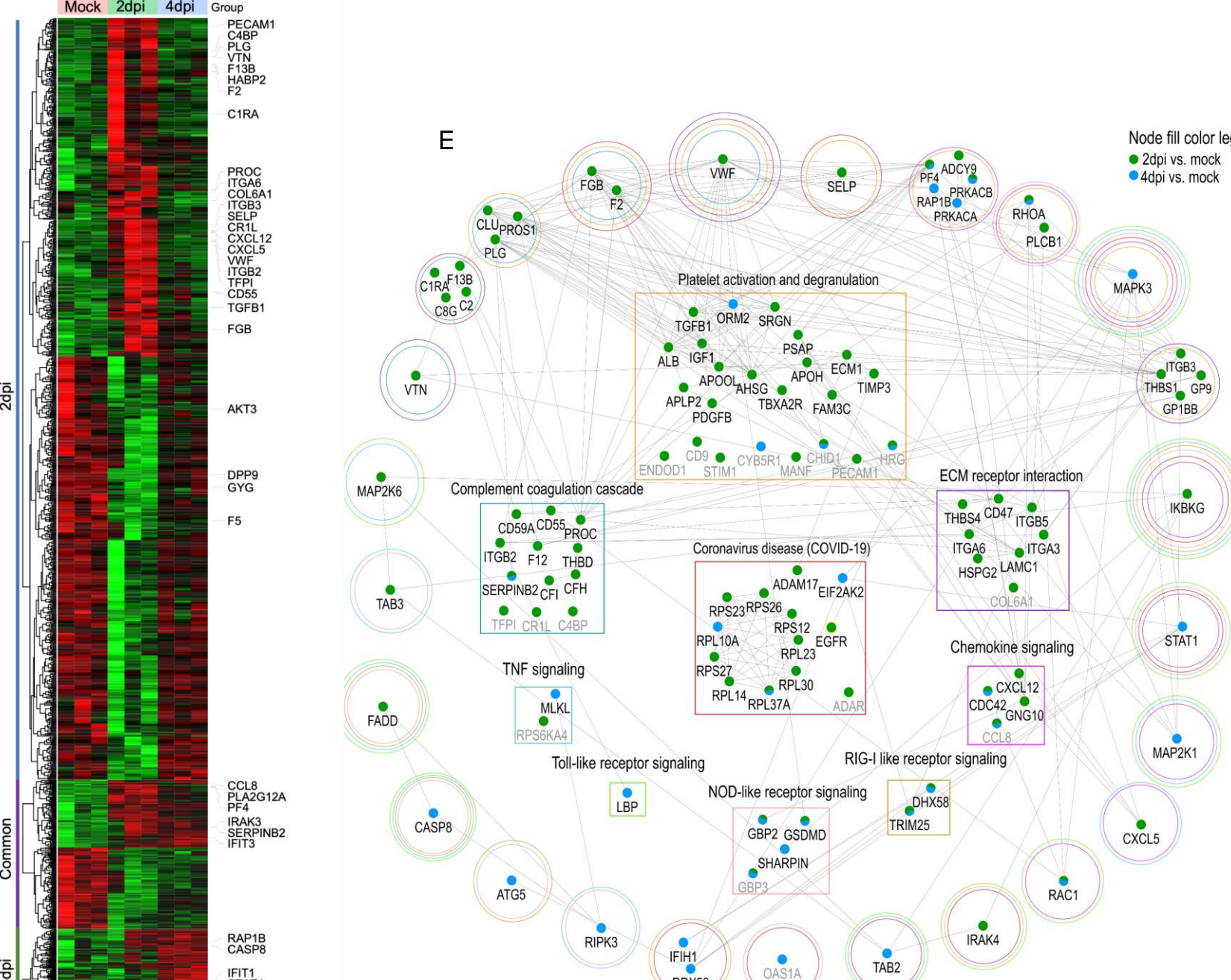
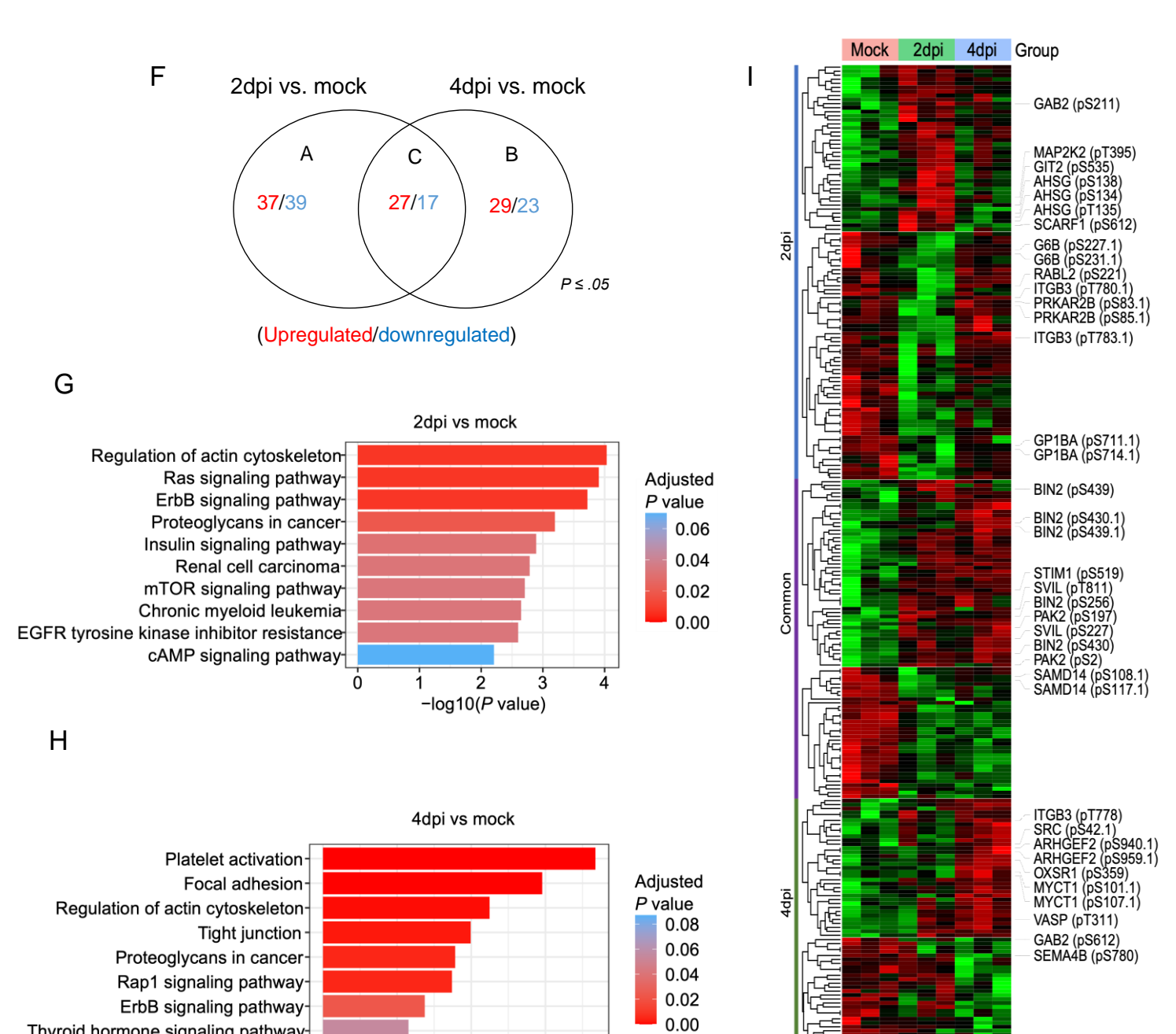


Figure 5. Distinct adaptations of platelet proteome and phosphoproteome during SARS-CoV-2 infection. K18-hACE2 mice were infected with SARS-CoV-2 (1×10^6 PFU) and circulating platelets were collected at 2dpi and 4dpi for quantitative proteome analysis by mass spectrometry. (A-C) Venn diagrams and (D, E) heatmaps of significantly regulated proteins and phosphites (unadjusted P \leq .05) in 2dpi versus mock, 4dpi versus mock or common for both time points. Raw normalized expression values (Z-score from -2/green to +2/red) and key proteins of interest are shown. (B, C; G, H) KEGG pathway enrichment analyses of significant (unadjusted P \leq .05) upregulated proteins and phosphites in 2dpi versus mock and 4dpi versus mock. (E) STRING-based protein-protein interaction network of differentially expressed proteins (unadjusted P \leq .05) linked to platelet activation and degranulation, complement-coagulation cascades, chemokine signaling, toll-like receptor signaling, TNF α signaling, Coronavirus disease (COVID-19), ECM receptor interaction, or NOD-like receptor signaling. Protein nodes differentially expressed in 2dpi versus mock are colored green, 4dpi versus mock are in blue, and those altered in both time-points are colored with both green and blue. Proteins in square boxes were enriched only in one pathway/process while proteins within circles were enriched in more than one pathway/process. Circle colors represent the different pathways/processes. All data shown (B-N) are based on quantitative proteomics. (E) We compared the SARS-CoV-2 infected mouse circulating platelets proteome data with human circulating platelets transcriptomic data from COVID-19 patients (published data set; Manne et al., Blood 2020). Pearson correlation analysis of 4-dpi mouse platelet proteome with human COVID-19 patients' platelets transcriptomic data set.

STRING-based protein-protein interaction network



Phosphoproteome



CD61 aggregates in SARS-CoV-2-infected humanized ACE2 mice

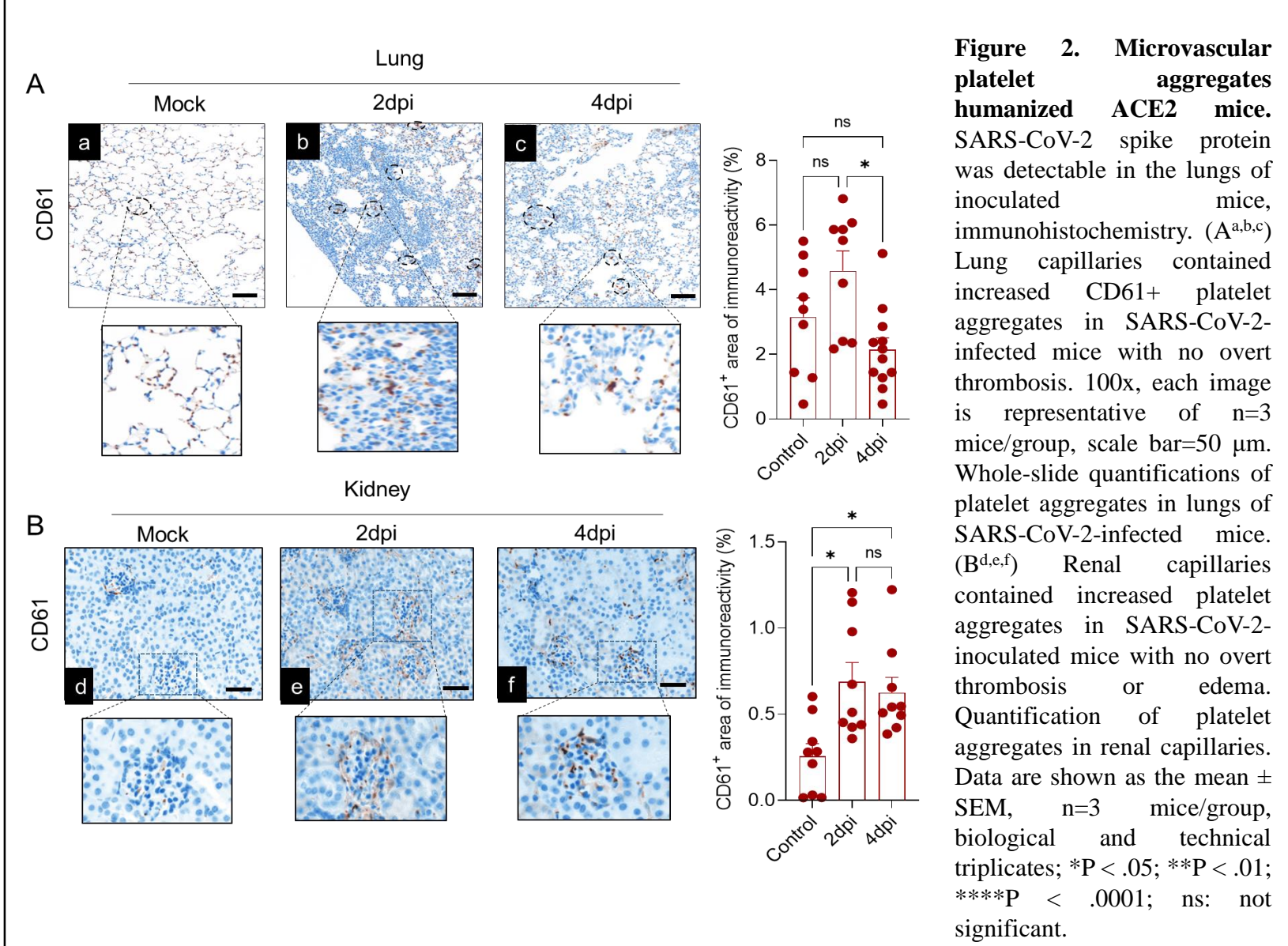


Figure 2. Microvascular platelet aggregates in SARS-CoV-2-infected humanized ACE2 mice. SARS-CoV-2 spike protein was detectable in the lungs of inoculated mice, immunohistochemistry. (A^{a,b,c}) Lung capillaries contained increased CD61+ platelet aggregates in SARS-CoV-2-infected mice with no overt thrombosis. 100x, each image is representative of n=3 mice/group, scale bar=50 μ m. Whole-slide quantifications of platelet aggregates in lungs of SARS-CoV-2-infected mice, (B^{a,b,c}) Renal capillaries contained increased platelet aggregates in SARS-CoV-2-inoculated mice with no overt thrombosis or edema. Quantification of platelet aggregates in renal capillaries. Data are shown as the mean \pm SEM, n=3 mice/group, biological and technical triplicates; *P < .05; **P < .01; ****P < .0001; ns: not significant.

Platelet Proteome Analysis

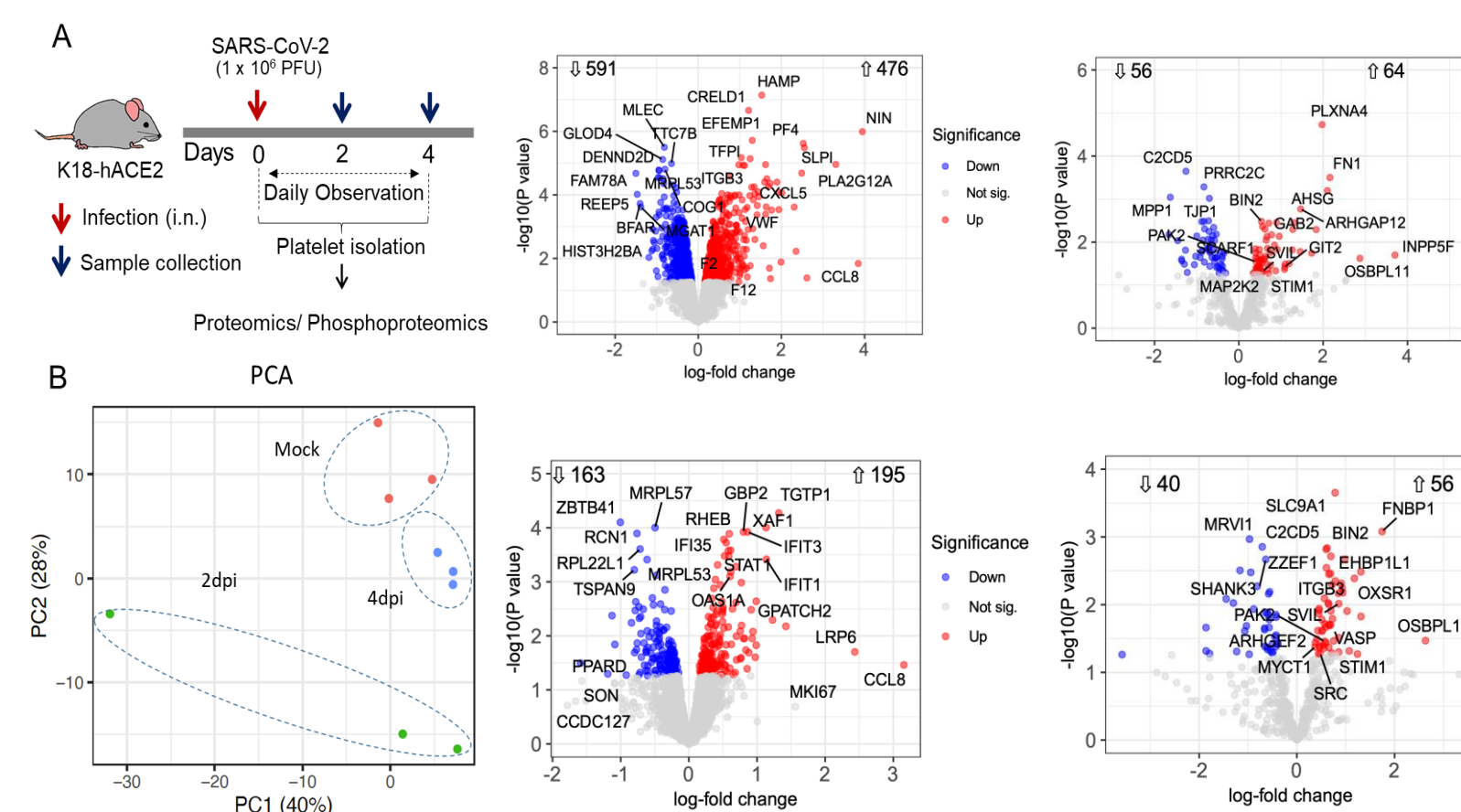


Figure 4. Platelet proteome analysis. (A) Experimental design. (B) Principal component analysis (PCA) plot and (C-F) Volcano plots of differentially expressed proteins (C, D) and phosphoproteins (E, F) detected in 2dpi versus mock and 4dpi versus mock quantitative proteomics datasets in K18-hACE2 mice (SARS-CoV-2, 1×10^6 PFU i.n.; biological triplicates). Numbers of significantly (unadjusted P \leq .05) up/downregulated proteins are shown.

Validation: Platelet lysates/plasma from SARS-CoV-2 infected mice

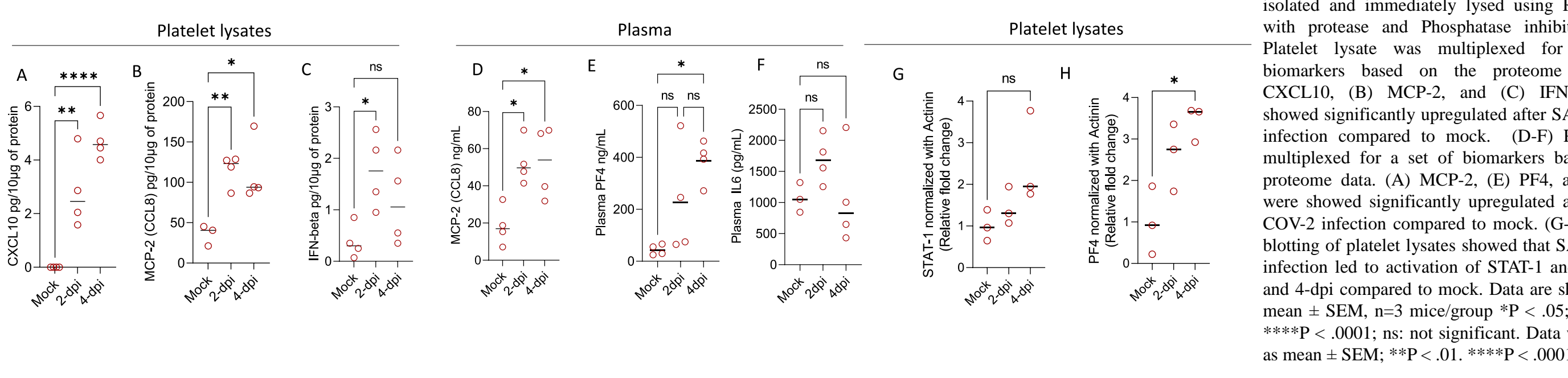


Figure 8. Correlation analysis of mouse proteome with human transcriptomic data from COVID-19 patients. We compared the SARS-CoV-2 infected mouse circulating platelets proteome data with human circulating platelets transcriptomic data from COVID-19 patients (published data set; Manne et al., Blood 2020). (E) Pearson correlation analysis of 4-dpi mouse platelet proteome with human COVID-19 patients' platelets transcriptomic data set.

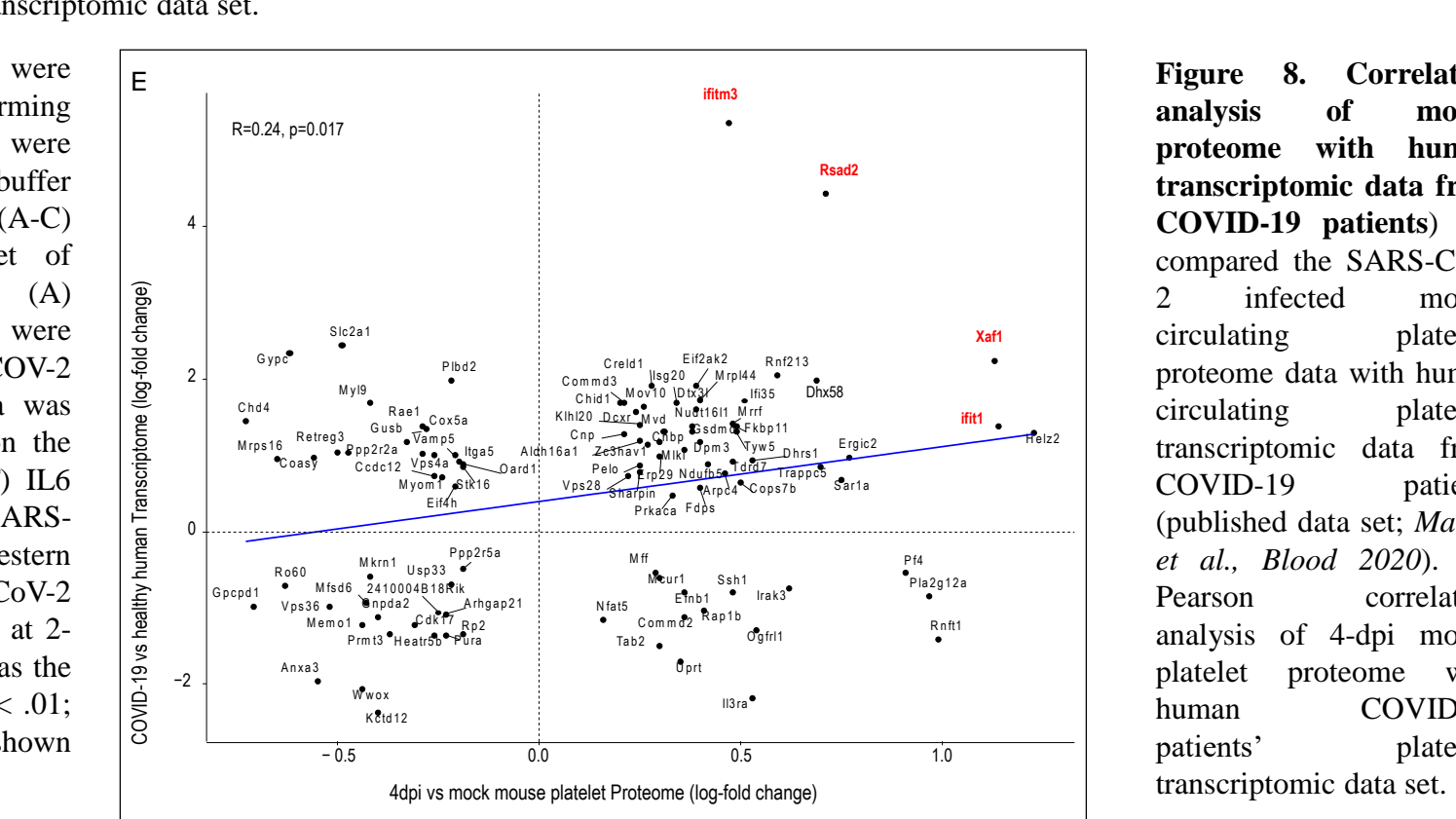


Figure 8. Correlation analysis of mouse proteome with human transcriptomic data from COVID-19 patients. We compared the SARS-CoV-2 infected mouse circulating platelets proteome data with human circulating platelets transcriptomic data from COVID-19 patients (published data set; Manne et al., Blood 2020). (E) Pearson correlation analysis of 4-dpi mouse platelet proteome with human COVID-19 patients' platelets transcriptomic data set.



Proteome and phosphoproteome analyses of SARS-CoV-2-infected humanized K18-ACE2 mice reveal hyperactive phenotype of circulating platelets

Saravanan Subramaniam, PhD

Pulmonary Center, Department of Medicine, School of Medicine, Boston University MA, USA

Bioactive and phosphoproteomic analyses reveal hyperactive phenotype of platelets in humanized K18-ACE2 mice infected with SARS-CoV-2

Saravanan Subramaniam¹, Ryan Matthew Hekman², Archana Jayaraman¹, Aoife Kateri O'Connell^{3,4}, Paige Montanaro^{3,5}, Devin Kenney^{3,4}, Maria Ericsson⁶, Sarah

Walachowski¹, Benjamin Blum², Katya Ravid^{7,8}, Nicholas A Crossland^{3,5}, Florian Douam^{3,4}, Andrew Emili², Markus Bosmann^{1,3,9}

¹Boston University, Department of Medicine, MA, USA; ²Center for Network Systems Biology, Boston, MA, USA; ³Boston University, National Emerging Infectious Diseases Laboratories (NEIDL), Boston, MA, USA; ⁴Boston University, Department of Microbiology, Boston, MA, USA

⁵Boston University, Department of Pathology and Laboratory Medicine, Boston, MA, USA; ⁶Electron Microscopy Core Facility, Harvard Medical School, Boston, MA, USA; ⁷Department of Medicine, Boston University School of Medicine, Boston, MA, USA; ⁸Whitaker Cardiovascular Institute, Boston University School of Medicine, Boston, MA, USA; ⁹Center for Thrombosis and Hemostasis, University Medical Center of the Johannes Gutenberg-University, Mainz, Germany



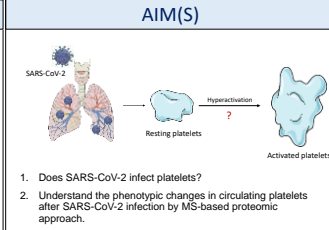
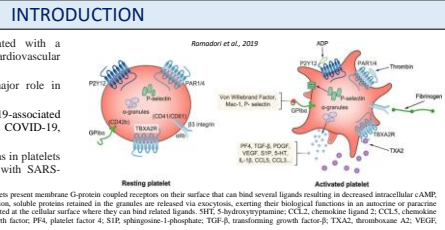
Boston University School of Medicine
Pulmonary Center

INTRODUCTION

- Coronavirus disease 2019 (COVID-19) is associated with a hypercoagulable state and increased incidence of cardiovascular complications.
- Platelets are effectors of hemostasis and play a major role in coordinating immune and inflammatory activities.
- Suitable animal models are needed to study COVID-19-associated coagulopathy (CAC) and platelet effector functions in COVID-19, which remain largely unclear.
- In our current study, we aimed to characterize alterations in platelets isolated from K18-hACE2 transgenic mice infected with SARS-CoV-2.

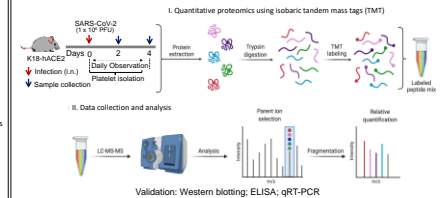
Schematic representation of a platelet in its resting state and upon activation. Upon activation, protein membrane G-proteins coupled receptors on their surface can bind several ligands resulting in decreased intracellular cAMP mobilization of Ca²⁺ stores and subsequent changes of cell morphology. Upon activation, soluble proteins retained in the granules are released via exocytosis, exerting their biological functions in an autocrine or paracrine manner. Similarly, membrane proteins retained in the granules are released when they can bind related ligands. **HTF**: 5-hydroxytryptamine; **CE2.1**: chemokine ligand 2; **CC1.5**: chemokine ligand 5; **GP1b**: glycoprotein 1b; **IL-1β**: interleukin-1β; **PDGF**: platelet-derived growth factor; **PF4**, platelet factor 4; **S1P**: sphingosine-1-phosphate; **TGF-β**: transforming growth factor-β; **TXA2**: thromboxane A2; **VWF**: von Willebrand factor; **ADP**: adenosine diphosphate

Resting platelet **Activated platelet**



1. Does SARS-CoV-2 infect platelets?
2. Understand the phenotypic changes in circulating platelets after SARS-CoV-2 infection by MS-based proteomic approach.

METHOD(S)



CONCLUSION(S)

- Abundance of SARS-CoV-2 spike protein in lungs of infected K18-hACE2 mice, but not in platelets and other organs (kidneys), suggests that platelet re-programming towards activation-degranulation-aggregation is likely attributable to a pneumonia-induced elevated circulatory factors (e.g. cytokines and thrombin)-driven response rather than direct platelet infection.
- Complement / coagulation pathways and a hyperactive platelet phenotype re dominant at 2-dpi and interferon signaling is dominant at 4-dpi.
- Circulating platelets in SARS-CoV-2 infected K18-hACE2 mice demonstrate a specific early hyperactive phenotype consistent with procoagulant platelets.

RESULTS

Clinical decline of SARS-CoV-2-infected humanized ACE2 mice

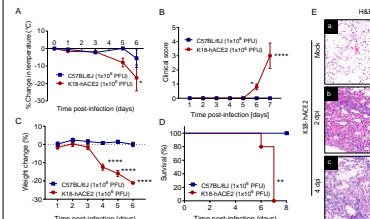


Figure 1. Clinical decline of SARS-CoV-2-infected humanized ACE2 mice. K18-hACE2 mice and CTRL mice were inoculated intranasally with 1x10⁷ plaque-forming units (PFU) or received saline mock. (A) % change in body temperature, (B) clinical score, (C) % change in body weight, and (D) survival were monitored. (E-F) Progressive interstitial pneumonia in K18-hACE2 mice at 2dpi and 4dpi with SARS-CoV-2. H&E staining. Data are shown as the mean ± SEM, n=5 mice/group. *P < .05; **P < .01; ***P < .001; ****P < .0001.

Invasive viral load and ultrastructural findings of lung cross sections

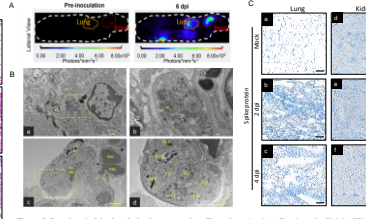


Figure 2. Microvascular platelet aggregates in SARS-CoV-2-infected mice. SARS-CoV-2 spike protein was detectable in the lungs of inoculated mice, immunohistochemically (A-F). Lung capillaries contained intraluminal CD61+ platelet aggregates in SARS-CoV-2-infected mice with no overt thrombosis. 100x, each image is representative of at least 3 mice/group, scale bar=50 μm. Whole-slide quantification of platelet aggregates in lungs of SARS-CoV-2-infected mice. (B-F) Lung capillaries contained increased platelet aggregates in SARS-CoV-2-infected mice with no overt thrombosis or edema. Quantification of platelet aggregates in renal capillaries. Data are shown as the mean ± SEM, n=3 mice/group. Biological and technical triplicates; *P < .05; **P < .01; ***P < .001; ****P < .0001, ns: not significant.

Proteome

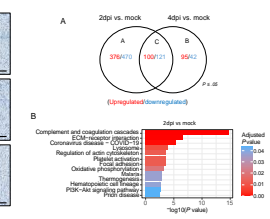


Figure 3. Platelet proteome analysis. (A) Experimental design. (B) Principal component analysis (PCA) plot and (C-F) volcano plots. Volcano plots of differentially expressed proteins. (C, D) and phosphoproteins. (E,F) detected in 2dpi versus mock and 4dpi versus mock quantitative proteomics datasets in K18-hACE2 mice (SARS-CoV-2, 1x10⁷ PFU i.n.), biological triplicates). Numbers of significantly (adjusted P < .05) up/downregulated proteins are shown.

STRING-based protein-protein interaction network

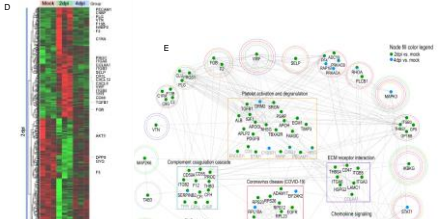


Figure 4. Distinct adaptations of platelet proteome and phosphoproteome during SARS-CoV-2 infection. K18-hACE2 mice were infected with SARS-CoV-2 (1x10⁷ PFU) and circulating platelets were collected at 2dpi and 4dpi for quantitative proteomics analysis by mass spectrometry. (A-F) Venn diagrams and (D,E) heatmaps of significantly regulated proteins and phosphoproteins (adjusted P < .05) in 2dpi versus mock. 4dpi versus mock for both time points. Raw normalized expression values (z-score from -2green to 2red) and key proteins of interests are shown. (B,C) G2H KEGG pathway enrichment analysis of significant (adjusted P < .05) upregulated proteins and phosphoproteins in 2dpi versus mock and 4dpi versus mock. (E) STRING-based protein-protein interaction network of differentially expressed proteins (analysis: 0.85) linked to platelet activation and degranulation, complement-coagulation cascades, thrombin signaling, PDGFR-1b receptor signaling, IL-1b receptor signaling, TNF signaling, TNF signaling, Coronavirus disease (COVID-19), HCM receptor interaction, NOD-like receptor signaling, Protein serine/threonine kinase signaling, and NOD-like receptor signaling. Proteins nodes differentially expressed in 2dpi versus mock are colored green, 4dpi versus mock are in blue, and those altered in both time-points are colored with both green and blue. Proteins in square boxes were enriched only in one pathway process while proteins within circles were enriched in more than one pathway process. Circle colors represent the different pathways processes. All data shown (B-F) are based on quantitative proteomics. (G) We compared the SARS-CoV-2 infected mouse circulating platelets proteome data with human circulating platelets transcriptomic data from COVID-19 patients (published data set; Monner et al., 2020). Pearson correlation analysis of 4-dpi mouse platelet proteome and human circulating platelets transcriptomic data set.

Phosphoproteome

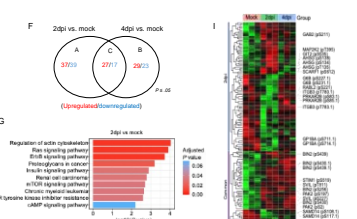


Figure 5. Correlation analysis of mouse proteome with human transcriptomic data from COVID-19 patients. We compared the SARS-CoV-2 infected mouse circulating platelets proteome data with human circulating platelets transcriptomic data from COVID-19 patients (published data set; Monner et al., 2020). (A) Pearson correlation analysis of 4-dpi mouse platelet proteome with human COVID-19 patients' platelets transcriptomic data set.

Validation: Platelet lysates/plasma from SARS-CoV-2 infected mice

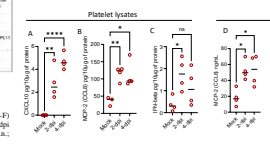


Figure 6. Biplaxial K18-hACE2 mice were inoculated intranasally with 1x10⁷ plaque-forming units (PFU) or received saline mock. Platelets were isolated and immediately lysed using RIPA buffer with protease and phosphatase inhibitors. (A-C) Platelet lysate was multiplexed for a set of biomarkers based on the proteome data. (A) MCP-2, (B) MCP-1, and (C) IL6 were shown significantly upregulated after SARS-CoV-2 infection compared to mock. (D-H) Western blotting of platelet lysates showed that SARS-CoV-2 infection led to activation of STAT1 and PF4. 2- and 4-dpi compared to mock. Data are shown as the mean ± SEM, n=3 mice/group. *P < .05; **P < .01; ***P < .001; ns: not significant. Data were shown as mean ± SEM. **P < .01; ***P < .001.

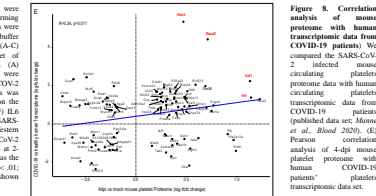
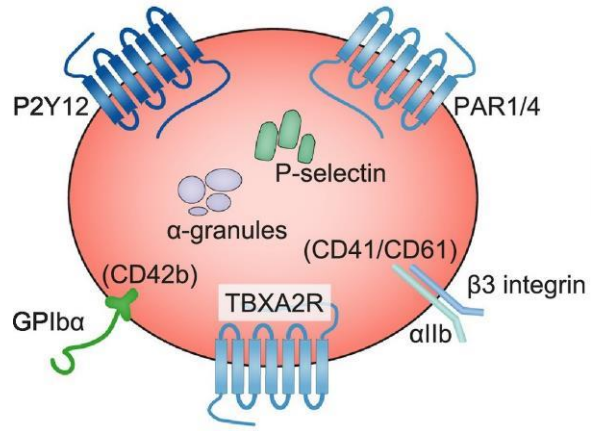
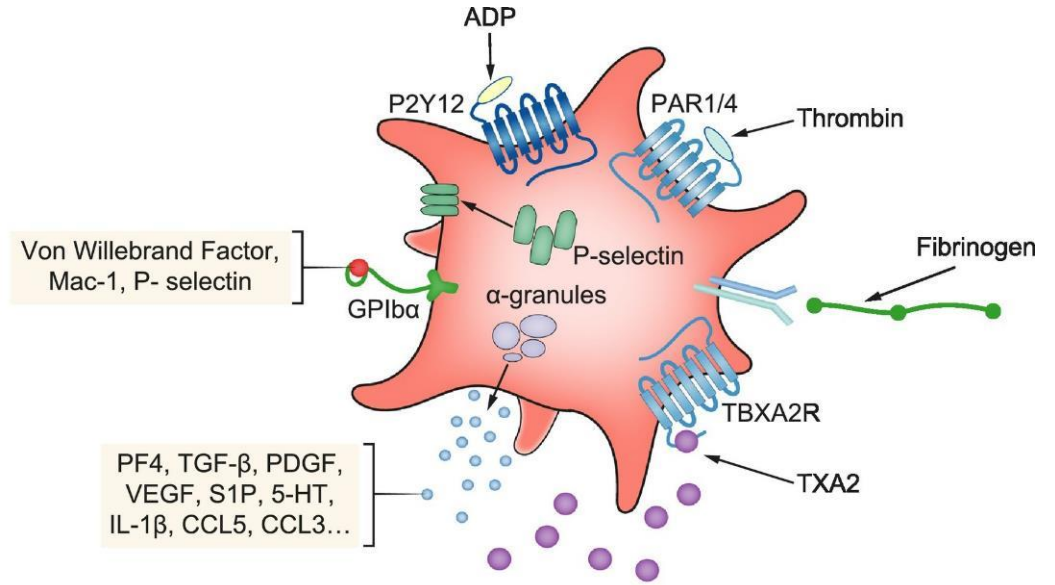


Figure 7. Correlation analysis of mouse proteome with human transcriptomic data from COVID-19 patients. We compared the SARS-CoV-2 infected mouse circulating platelets proteome data with human circulating platelets transcriptomic data from COVID-19 patients (published data set; Monner et al., 2020). (A) Pearson correlation analysis of 4-dpi mouse platelet proteome with human COVID-19 patients' platelets transcriptomic data set.

Platelets

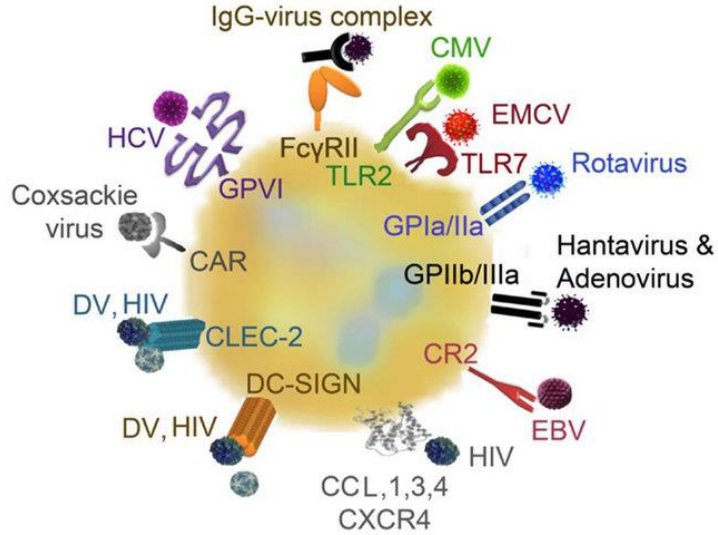


Resting platelet



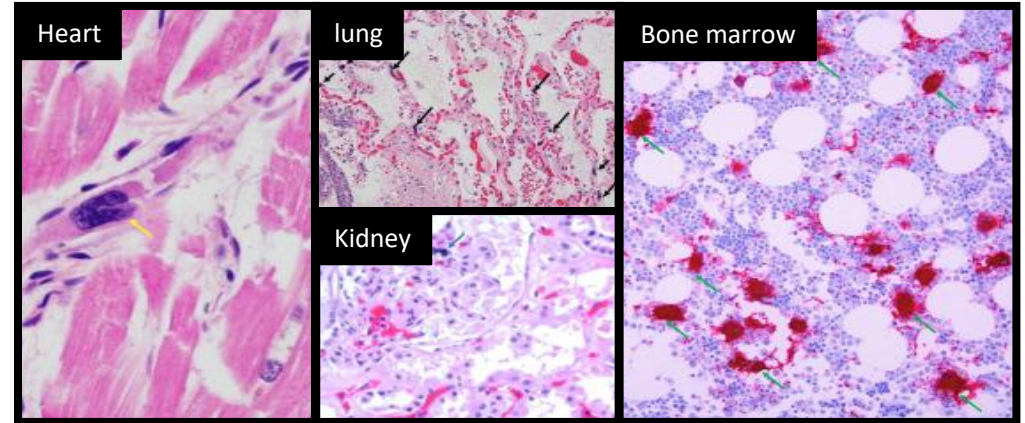
Activated platelet

Platelets and viruses



Autopsies (females) – COVID-19

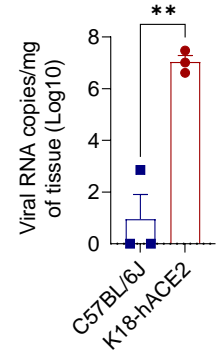
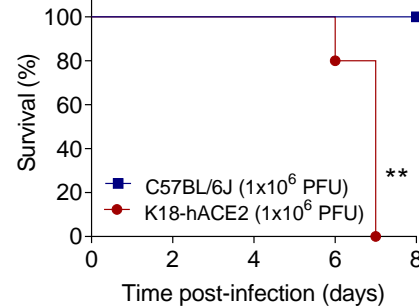
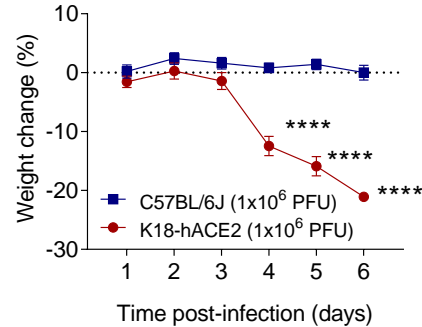
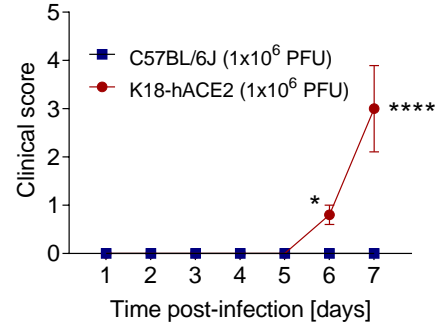
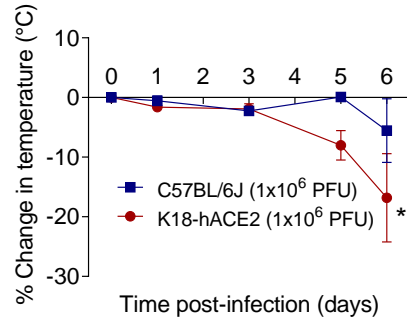
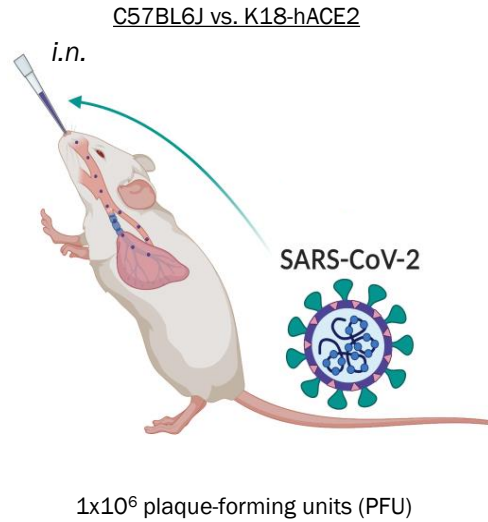
Rapkiewicz, et al., LANCET, 2020



Hematoxylin and Eosin staining (Megakaryocytes and platelets are highlighted by CD61 staining)

1. Does SARS-CoV-2 infect platelets?
2. Understand the phenotypic changes in circulating platelets after SARS-CoV-2 infection

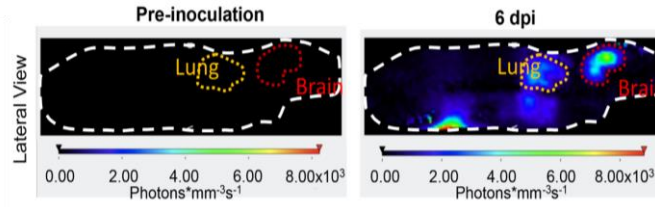
Clinical decline of SARS-CoV-2-infected humanized ACE2 mice



“hACE2 is required for SARS-COV-2 infection in mice”

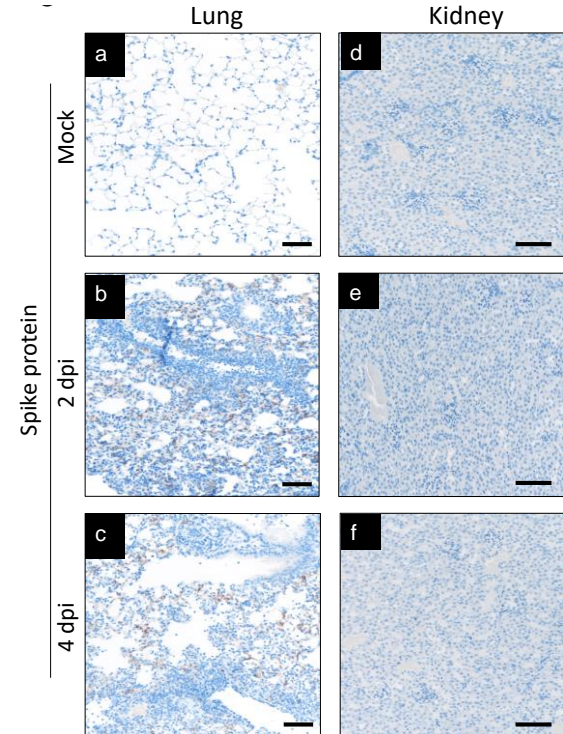
Invasive viral load and ultrastructural findings of lung cross sections

In vivo 3D-imaging

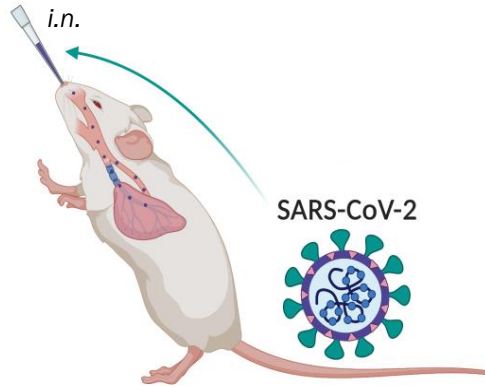


Carossino, et al., Viruses, 2022

Immunohistochemistry



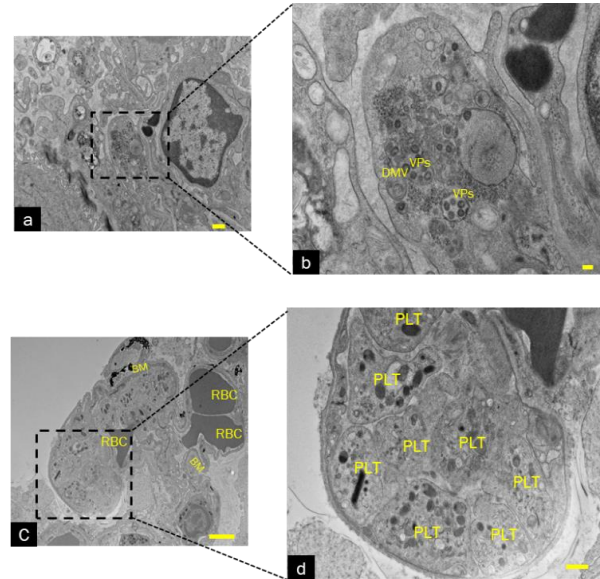
K18-hACE2



1x10⁶ plaque-forming units (PFU)

Mock - 2 dpi - 4 dpi - 6 dpi

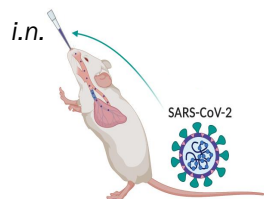
Transmission electron microscopy (TEM)



Live virus in lungs and brain, but not in other major organs

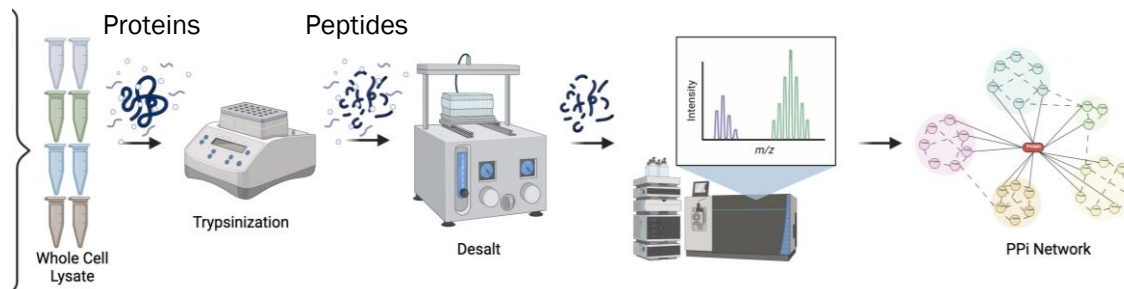
Proteome and Phosphoproteome analyses of SAR-CoV-2 infected K18-hACE2 mice

Mock – 2 dpi – 4 dpi

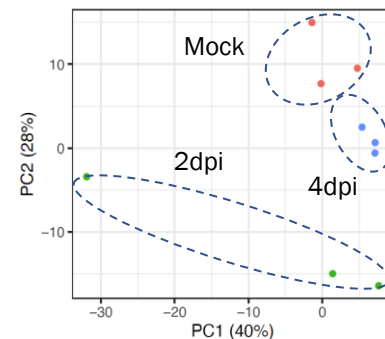


1×10^6 PFU

K18-hACE2 mice



PCA

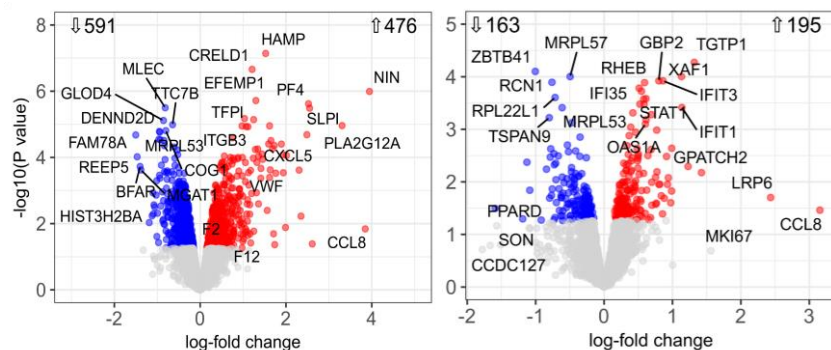


Proteome

Phosphoproteome

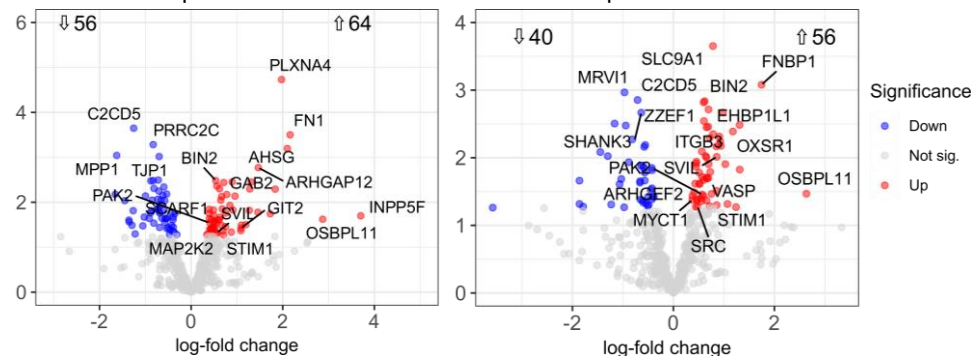
2 dpi vs. mock

4 dpi vs. mock



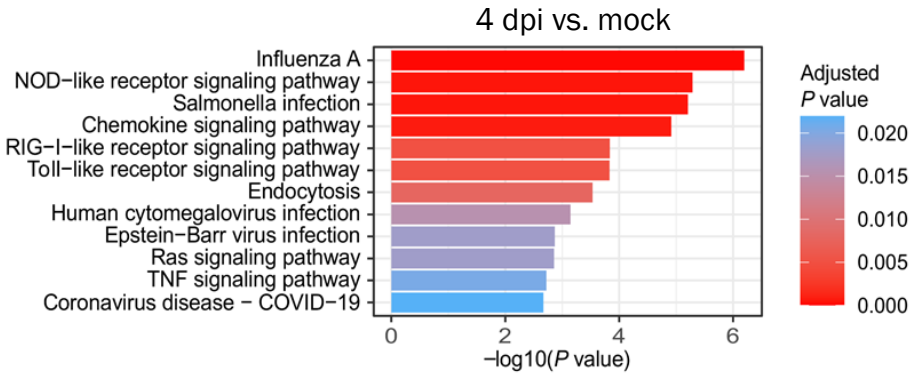
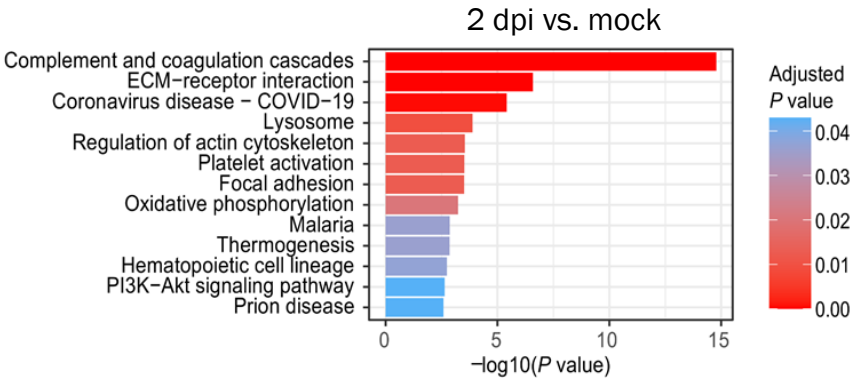
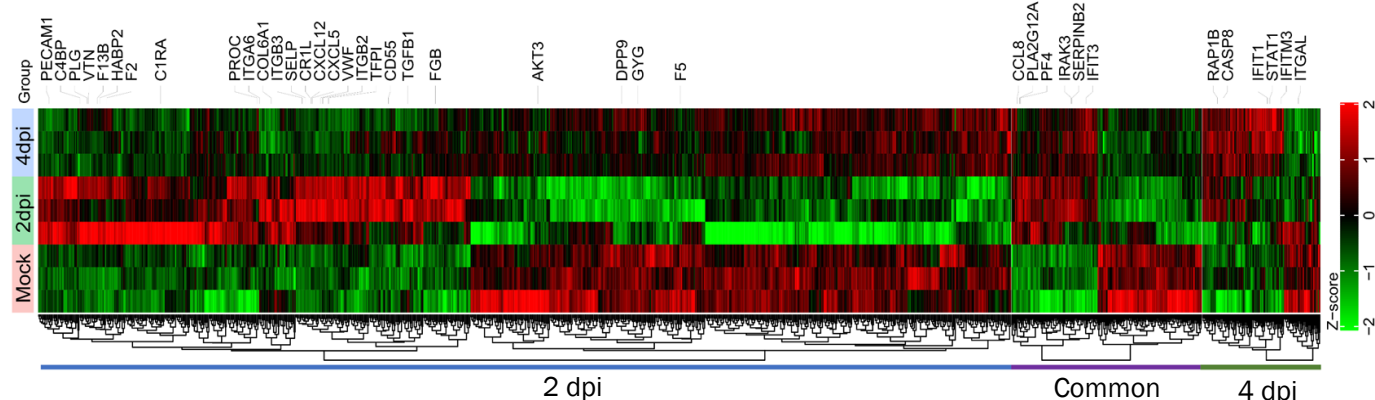
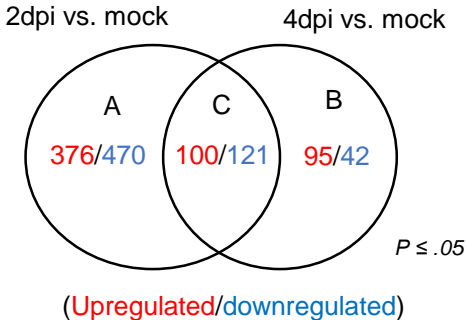
2 dpi vs. mock

4 dpi vs. mock

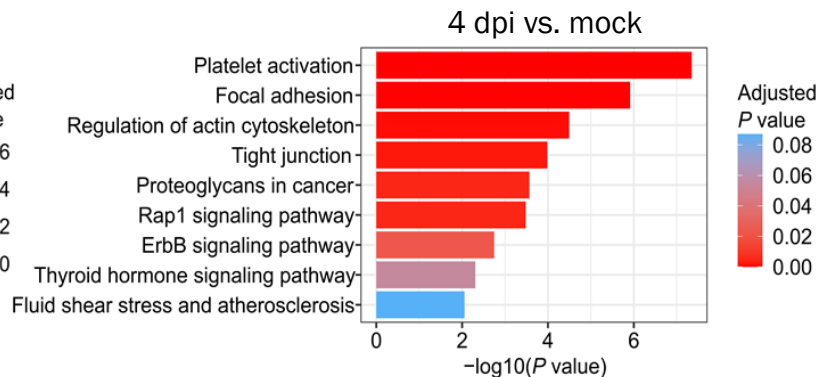
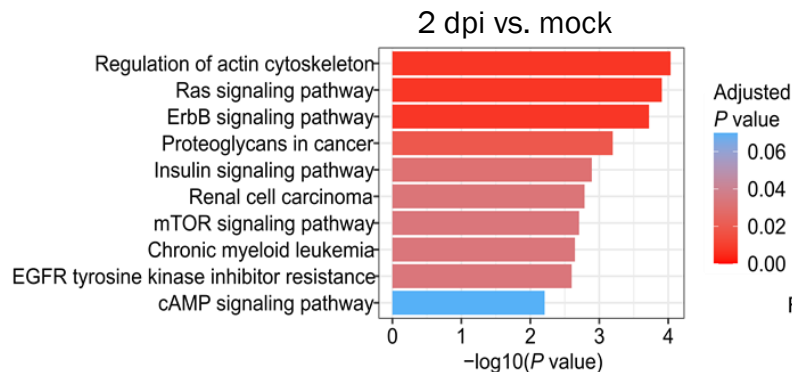
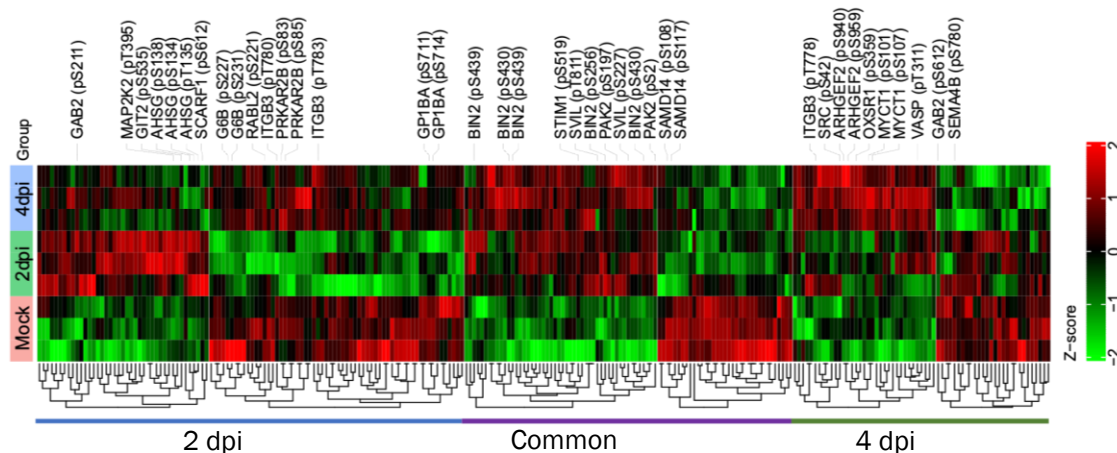
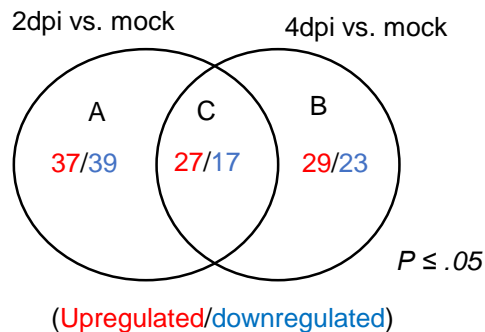


Significance
 ● Down
 ● Not sig.
 ● Up

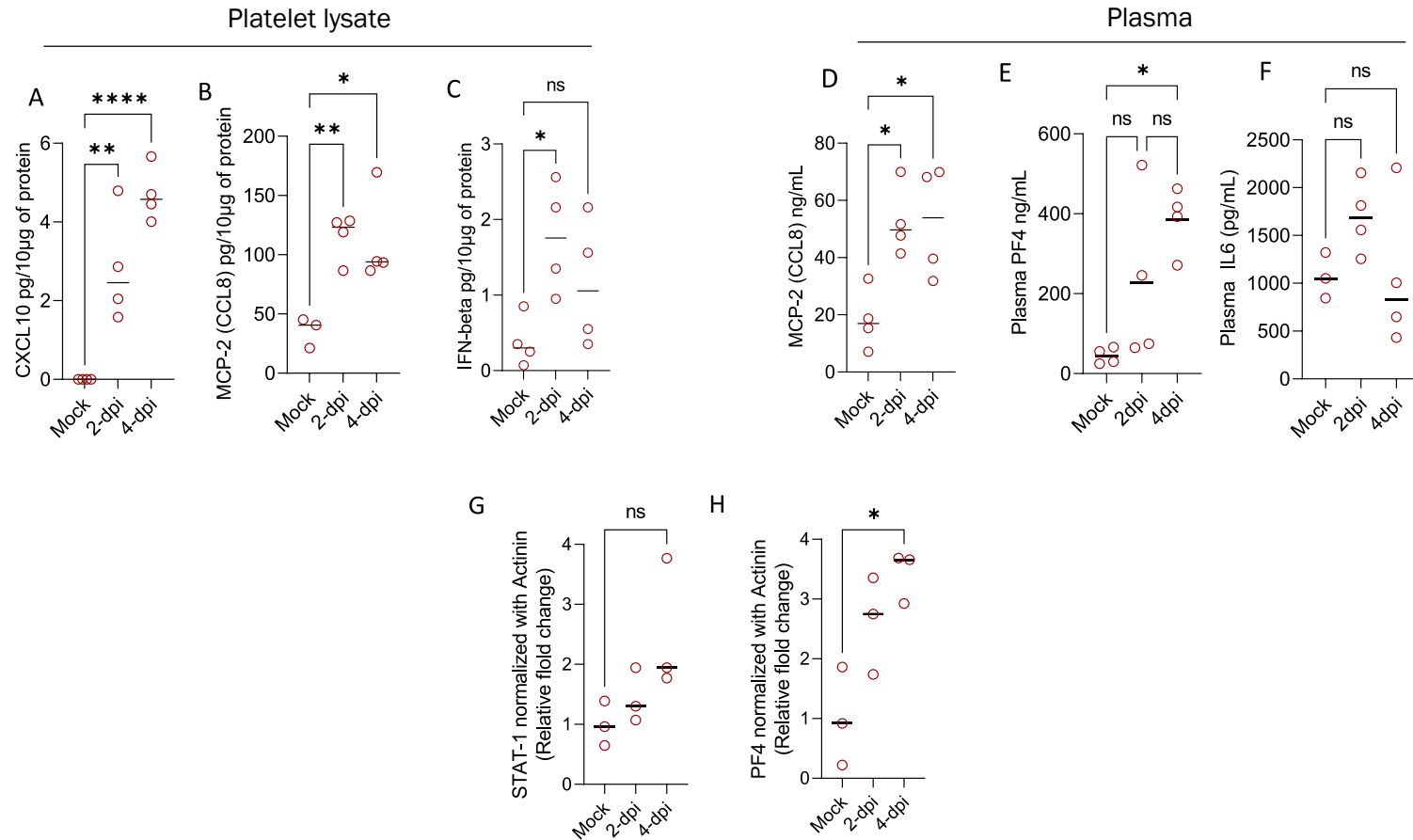
Distinct expression of proteins in circulating platelets after SARS-CoV-2 infection



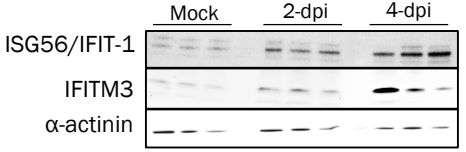
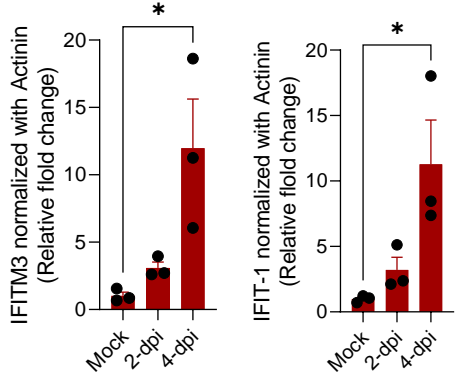
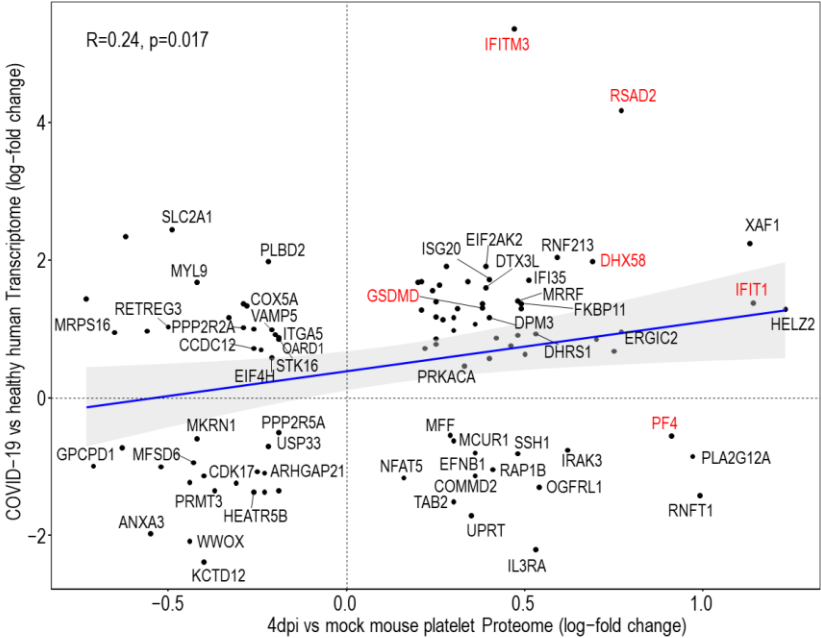
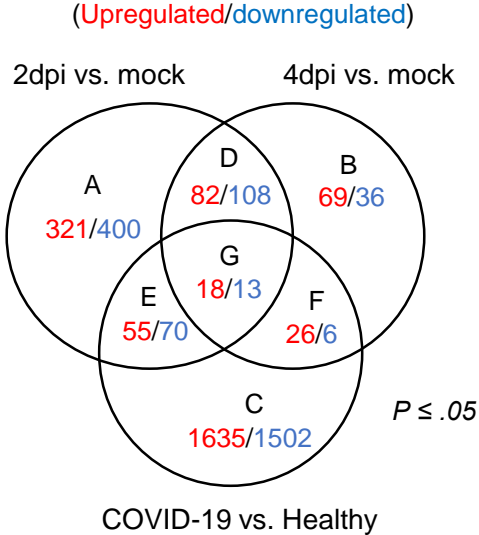
Distinct expression of Phosphoproteins in circulating platelets after SARS-CoV-2 infection



Validation: Platelet lysate/plasma from SARS-CoV-2 infected mice

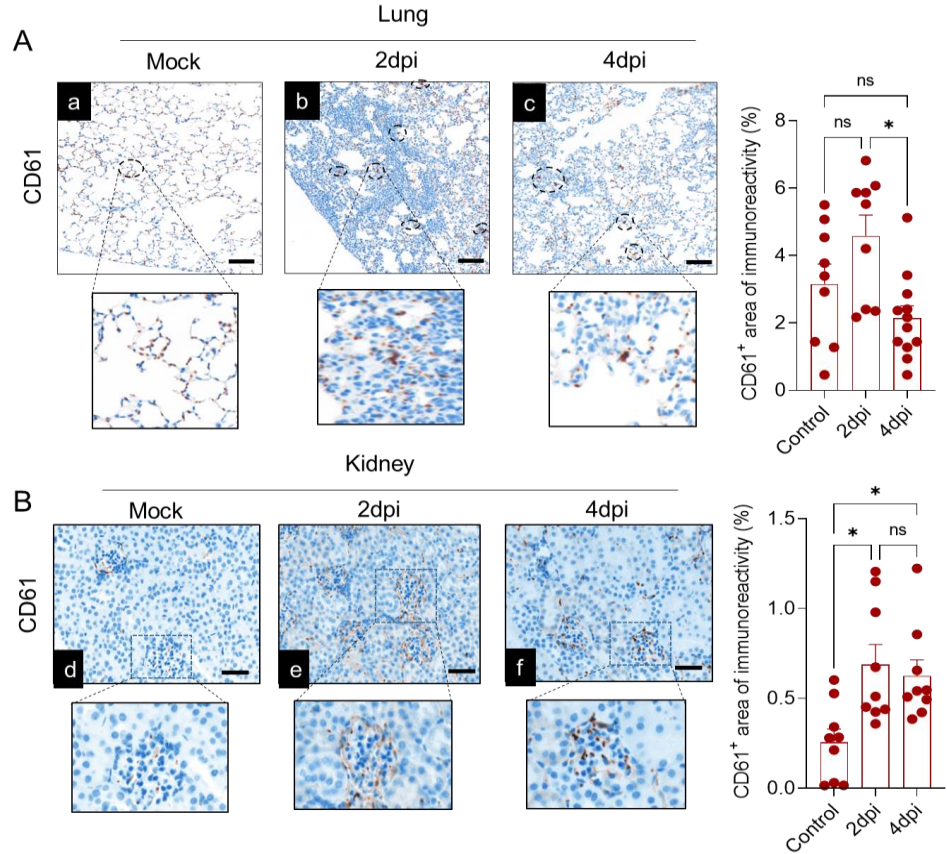
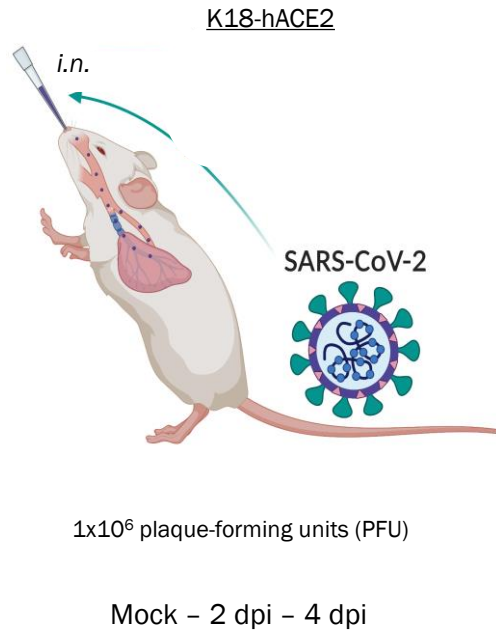


Correlation: Mouse proteome Vs. Human transcriptome

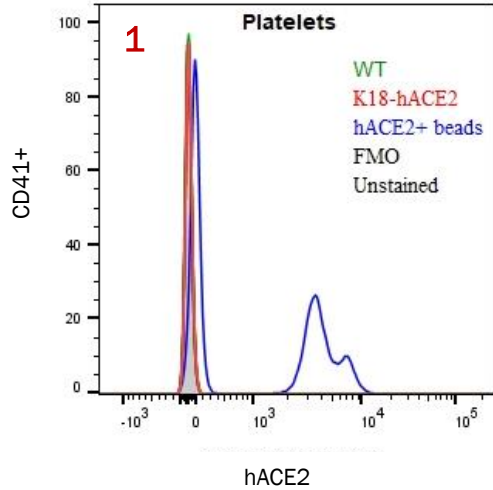


K18-hACE2 mouse can serve as a good animal model to study COVID-19 associated coagulation and immune responses.

CD61 (Integrin B3) aggregates in SARS-CoV-2-infected humanized ACE2 mice

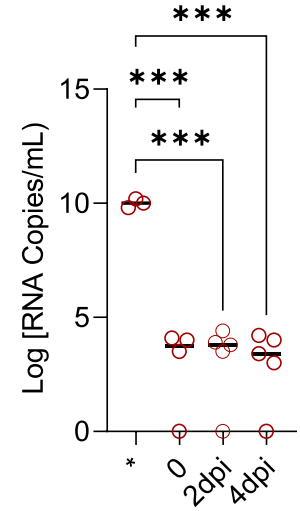
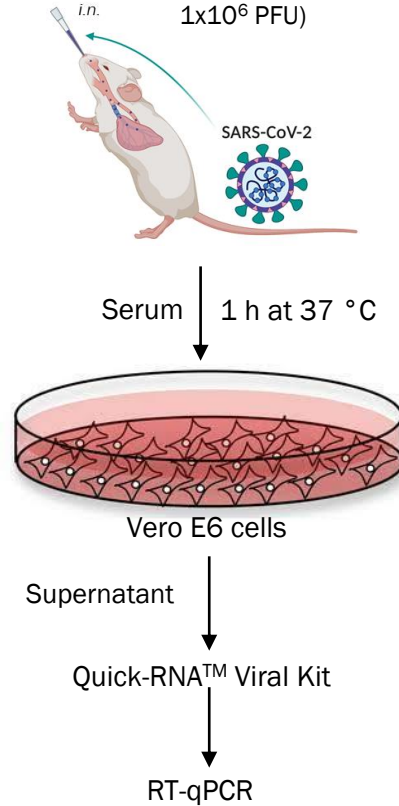


Serum infectivity assay of Vero E6 cells



K18-hACE2 mouse platelets do not express hACE2 receptor

Mock - 2 dpi - 4 dpi



“No detectable infectious viral particles in the serum”

Carossino et al., Viruses, 2022

Conclusions

- our in vivo proteome analysis showed **no detectable direct SARS-CoV-2 infection of platelets (early time points)** in K18-hACE2 mice.
- SARS-CoV-2 infected K18-hACE2 mice showed **early platelet activation-adhesion-degranulation markers**.
- **Complement-coagulation cascades** and hyperactive platelet phenotype were dominant **at 2-dpi** and **interferon signaling** was dominant **at 4-dpi**.
- Abundance of SAR-CoV-2 **spike protein in lungs but not in platelets and other organs (kidney), as well as lack of hACE2 on K18-hACE2 mouse platelets**, suggests that platelet re-programming towards activation-degranulation-aggregation is likely attributable to **pneumonia-induced other factors (such as, cytokines, thrombin)-driven response rather than direct platelet infection**.

Acknowledgements

Pulmonary Center, Department of Medicine, School of
Medicine, Boston University MA, USA

Dr. Markus Bosmann

Archana Jayaraman

Sarah Walachowski

Center for Network Systems Biology, Boston University,
Boston, MA, USA

Prof. Andrew Emili

Ryan Matthew Hekman

Benjamin Blum

Electron Microscopy Core Facility, Harvard Medical
School, Boston, MA, USA

Dr. Maria Ericsson

National Emerging Infectious Diseases Laboratories (NEIDL),
Boston University, Boston MA, USA

Dr. Florian Douam

Aoife Kateri O'Connell

Devin Kenney

Dr. Nicholas Crossland

Mary Paige Montanaro

Department of Medicine, Boston University School of Medicine,
Boston, MA, USA

Whitaker Cardiovascular Institute, Boston University School of
Medicine, Boston, MA, USA

Prof. Katya Ravid